ELSEVIER

S0032-3861(96)00539-3

Polymer Vol. 38 No. 3, pp. 571–576, 1997

0032-3861/97/$17.00+0.00

An extended nonlinear mechanical model for solid-filled Mooney–Rivlin rubber composites

Chao-Hsun Chen* and Yu-Chung Wang
Institute of Applied Mechanics, National Taiwan University, Taipei, Taiwan
(Received 3 August 1995; revised 29 March 1996)

This paper studies experimentally the creep behaviour of particle-reinforced Mooney–Rivlin rubber composites (PR-MRC). The specimens were made of hydroxyl-terminated polybutadiene (HTPB) cured with toluene-2,4-diisocyanate (TDI) as the matrix, and contained 0 to 40% volume fraction (f_1) of inclusions. They were subjected to uniaxial tensile and constant-loading creep tests. Results show that the material behaviour does indeed display the characteristics of Mooney–Rivlin material and that Eyring's reaction rate principle is suitable to describe the viscoelastic behaviour of this rubber composite. Hence, the Boltzmann superposition technique cannot be applied to solve the creep problems of these rubber composites. Although Findley *et al.* (1976) have proposed the multiple integrals form, solving this form is complicated and does not guarantee convergence. In order to describe the creep behaviour of Mooney–Rivlin rubber composites, we have extended the So–Chen formulation of the nonlinear four-element Burger's (NFEB) model, which describes the nonlinear stress–strain relationship of neo-Hookean rubber elasticity. This avoids the above-mentioned difficulty and an analytic solution is obtained, which is in good agreement with the experimental results.

(Keywords: nonlinear; particle-reinforced; Mooney–Rivlin; rubber; composites; creep; four-element Burger's model; rubber elasticity)

INTRODUCTION

Composites are widely used because of their increased material toughness, strength, impact resistance, etc., which have been proven to suit our engineering needs. The rubber matrix itself exhibits viscoelastic behaviour. Therefore, the stress and strain of solid-filled rubber composites are a function of time.

Although linear viscoelastic material is completely described in continuum mechanics literature[1–3], the simplest way to represent the stress–strain and time integral is to employ the Boltzmann superposition method, in which the time–function relation between compliance and relaxation modulus refers to the mechanical response as related to the loading history, and then to superimpose each individual effect of these small time intervals to form the integral representation. The differential representation of time-varying stress–strain is to superimpose the linear spring and the Newton dashpot to form the mechanical model; examples are the Maxwell model, Kelvin model, four-element Burger's model, generalized Maxwell model. These models can be used to analyse the mechanical behaviour linking differential time and stress or strain. The reason that these representations are often popularly used in experiments is because the material constants determined from creep experiments can well describe the mechanical behaviour of the material.

For nonlinear viscoelastic material the stress–strain relationship is still nonlinear, even under very small strain conditions. The Boltzmann superposition method can no longer be applied. To extend this method, Findley *et al.*[4] directly expanded the nonlinear integral to multiple integral representation form, and Rivlin derived from this the constitutive relation of material with memory. They employed the continuum mechanics methods[5,6], and encountered the difficulty of convergency of the multiple integrals. Schapery[7] employed thermodynamics to derive a simple integral form by adding a nonlinear modified term to describe the nonlinear stress–strain relationship, and successfully reduced this back to the linear relation. Furthermore, suitable nonlinear elements can be found to form nonlinear mechanical models, such as the So–Chen nonlinear four-element Burger's (NFEB) model[8], which can well describe nonlinear mechanical behaviour. Each individual molecular chain is treated as the 'entropy spring' and the rubber elasticity formula is employed to replace the linear spring. Also, from the concept of nonlinear activation energy jump over the energy barrier, the Eyring activation energy dashpot can be used to replace the Newton dashpot.

The main theme of this paper is to study the viscoelastic behaviour of solid-filled Mooney rubber composites, using hydroxyl-terminated polybutadiene (HTPB) rubber composites filled with glass beads or graphite to simulate the viscoelastic behaviour of this type of composite. We have extended the So–Chen

* To whom correspondence should be addressed

NFEB model[8] to describe the nonlinear stress–strain relation of Mooney–Rivlin rubber elasticity.

MOONEY–RIVLIN RUBBER ELASTICITY AND THE ASSOCIATED SECANT MODULI

Let λ_i be the principal deformation stresses associated with the Cauchy–Green deformation tensor. For a Mooney–Rivlin material characterized by two constants a_1 and a_2, the principal Cauchy stress components τ_k are determined[9] by

$$\tau_k = 2\left(\tau_k^2 \cdot a_1 - \frac{a_2}{\lambda_k^2}\right) + p, \quad k = 1.2,3 \tag{1}$$

where P is an unknown hydrostatic stress. The above equation is augmented by the constant volume constraint relation

$$\lambda_1\lambda_2\lambda_3 = 1 \tag{2}$$

Consider now the following generalized tensile loading

$$\tau_3 = P, \quad \tau_2 = \tau_1 = Q \tag{3}$$

where Q vanishes for a simple tensile loading. It follows from equations (1) and (2) that the associated deformation is

$$\lambda_3 = \Lambda = -\frac{a_2}{4a_1} - \frac{M}{4\sqrt{3}a_1\sqrt{A}} + \frac{\sqrt{|N| + B}}{a_1\sqrt{24AM}} \tag{4}$$

where

$$M = (2R^2a_1 - 72a_1^2a_2 + 4Ra_1A + 3a_2^2A + 2a_1A^2)^{1/2}$$

$$A = (-R^3 + 108a_1^3 - 162Ra_1a_2 - 108a_2^3 + L)^{1/3}$$

$$L = 2\sqrt{27}[108(a_1^3 + a_2^3)^2 + (2R^3 + 324a_1a_2R)(a_2^3 - a_1^3) + R^2a_1a_2(207a_1a_2 + 4R^2)]^{1/2}$$

$$B = \frac{M}{2}(12Ra_1A + 9a_2^2A - M^2)$$

$$N = \sqrt{27}A^{3/2}(2Ra_1a_2 + a_2^3 - Ba_1^3) \tag{5}$$

$$\lambda_1 = \lambda_2 = \Lambda^{-1/2} \tag{6}$$

and

$$R = \left(\lambda_3^2 - \frac{1}{\lambda_3}\right)\left(2a_1 + \frac{2a_2}{\lambda_3}\right) \tag{7}$$

$$R = P - Q \tag{8}$$

It is clear from the above that the desired material constants a_1 and a_2 may be deduced by fitting equation (4) to an experimentally measured curve for the simple tension test

$$R = P = \tau_3, \quad Q = 0 \tag{9}$$

Recalling that the three principal engineering strains ϵ_{KK} are related to the principal stretches by $\epsilon_{KK} = \lambda_k = 1$, we have

$$\epsilon_3 = e(R) = \Lambda(R) - 1 \tag{10}$$

$$\epsilon_1 = \epsilon_2 = e_T(R) = \Lambda^{-1/2}(R) - 1 \tag{11}$$

The generalized tensile loading (equation (3)) and the above calculated strains may be made to satisfy the following linear elasticity relations

$$\epsilon_3 = \frac{1}{E}[\tau_3 - \upsilon(\tau_1 + \tau_2)]$$

$$\epsilon_1 = \frac{2}{E}[\tau_1 - \upsilon(\tau_2 + \tau_3)] \tag{12}$$

$$\epsilon_2 = \frac{1}{E}[\tau_2 - \upsilon(\tau_1 - \tau_3)]$$

where E and υ are the so-called secant moduli associated with P and Q, i.e.

$$E = \frac{R(R + 3Q)}{R[\Lambda - 1] + 2Q[\Lambda - \Lambda^{-1/2}]} \tag{13}$$

$$\upsilon = \frac{R[1 - \Lambda^{-1/2}] + Q[\Lambda - \Lambda^{-1/2}]}{R[\Lambda - 1] + 2Q[\Lambda - \Lambda^{-1/2}]} \tag{14}$$

E and υ are the secant Young's modulus and secant Poisson's ratio, respectively. Secant shear modulus μ and secant bulk modulus κ follow from the usual definitions. We have

$$\mu = \frac{1}{2}\frac{R}{\Lambda - \Lambda^{-1/2}} \tag{15}$$

$$\kappa = \frac{1}{3}\frac{R + 3Q}{\Lambda + 2\Lambda^{-1/2} - 3} \tag{16}$$

EXPERIMENTAL

The specimens used in the uniaxial tensile creep tests were made of hydroxyl-terminated polybutadiene (HTPB) cured with toluene-2,4-diisocyanate (TDI) as the matrix, compounded with glass beads and graphite in volume fractions (f_1) ranging from 0% to 40%. Their individual properties are as follows. HTPB rubber: Poisson ratio 0.499; Young's modulus (E) 1.96 MPa; shear modulus (G) 0.654 MPa. Glass beads (from Toshiba-Ballotini Co., Japan): diameter 66–88 μm; Poisson ratio 0.24; Young's modulus (E) 68 500 MPa; Shear modulus (G) 27 600 MPa. Graphite: density 1770 kg m^{-3}; Young's modulus (E) 10 072 MPa; shear modulus (G) 4200 MPa; aspect ratio 0.15.

Tensile specimens with gauge lengths of 20 mm in accordance with ASTM D412 were cut from sheets. All specimens were kept in a desiccator for 15 days for post-curing and to stabilize their properties. They were then used in creep tests under constant load. All the tensile tests and creep tests were performed in a laboratory environment of 50% relative humidity (r.h.) at 25°C.

MECHANICAL BEHAVIOUR AND MODEL ANALYSIS

Since the polymer matrix itself is dependent on strain rate and time, the influence of different volume fractions of inhomogeneities on its tensile strength and creep behaviour becomes very important. This section describes rubber elasticity and the Eyring reaction rate principle derived from the deformation of the micro-molecular chain under stresses; first, the theory of molecular jumping velocity between two energy steps is recapitulated before being applied to construct the NFEB model.

Stress–strain relation

The smaller the strain rate that the specimen undergoes, the shorter the elongation which the specimen can take before it fractures. Also, the tensile strength and elongation increase as the strain rate increases. The stress–strain curves show that even under a very small strain condition this material still exhibits a very strong nonlinear relation; therefore, the linear mechanical model cannot be applied to describe the mechanical behaviour of this material.

For convenience of measurement in a simple tension test, we need to use the relation between the engineering stress σ and true stress (Cauchy stress) τ_3 as

$$\sigma = \tau_3(1 + \epsilon_{11})(1 + \epsilon_{22}) \tag{17}$$

The engineering stress σ and engineering strain ϵ_{33} are defined as follows

$$\sigma = \frac{p}{A_0} \tag{18}$$

$$\epsilon_{33} = \mathrm{e} = \frac{L - L_0}{L_0} \tag{19}$$

where A_0 is the original cross-section area, L_0 and L are the length before and after deformation, respectively, and P is the applied force on the specimen.

Figure 1 shows typical stress–strain results for PR-MRC. These show that stiffness increases with the amount of particles used for reinforcement, and suggest that the interfacial bonding strength of PR-MRC is from molecular chains across the solid particles. Thus the presence of the inclusions restricts the lateral contraction of the matrix, and so increases the stress in the stretched direction. The typical numerical solutions of engineering stress σ vs e curves shown in *Figure 1* are in very good agreement with experimental results. They show that the stress–strain curve of the numerical solution coincides with the asymptotic solution (equation (7)). The two material constants a_1 and a_2, determined by fitting equation (7), are tabulated in *Table 1*.

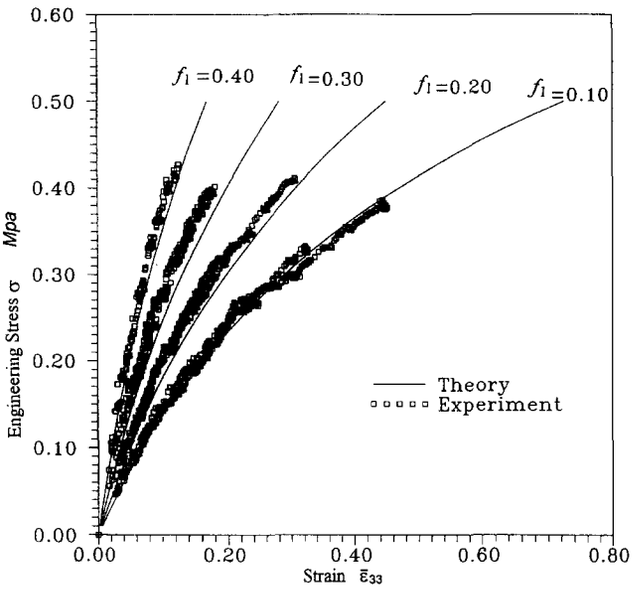

Figure 1 Engineering stress σ vs strain $\bar{\epsilon}_{33}$ for different volume fractions of glass-bead-reinforced HTPB rubber composites

Table 1 The material constants for equation (7)

Volume fraction f_1 for glass-bead-reinforced HTPB (%)	a_1	a_2
10	−0.02	0.31
20	−0.18	0.60
30	−0.61	1.23
40	−1.26	2.14

Creep behaviour of PR-MRC

Creep behaviour. The creep loading machine shown in *Figure 2* is used to determine the creep strain–time relation under constant loading. *Figure 3* shows that

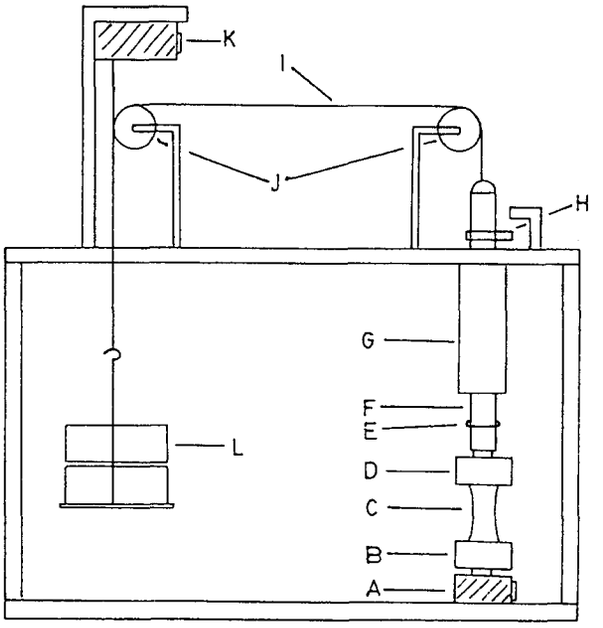

Figure 2 Creep testing machine: A, load cell; B, lower clip; C, specimen; D, upper clip; E, stop ring; F, moving bar; G, cylindrical shell; H, displacement transducer lower clip; I, wire; J, roller; K, displacement transducer; L, weight

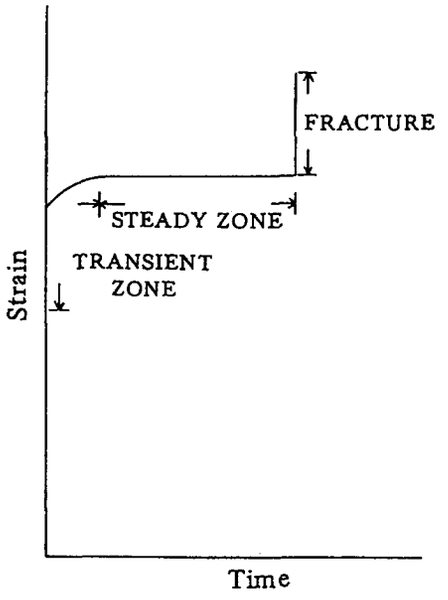

Figure 3 Creep history diagram

the creep history can be distinguished into three stages as follows:

(a) *Transient stage:* After the initial stretch, the slippage of the molecular chain changes from very obvious to steady state. The strain rate therefore starts from a maximum value and reduces to a constant value. Here we call this stage the first stage of creep.

(b) *Steady stage:* When the slippage of the molecular chain reaches a steady state, the whole molecular structure also reaches thermodynamic equilibrium and the strain rate is almost constant. We call this the second stage of creep.

(c) *Fracture stage:* At this stage the material fractures with no advance symptom.

Nonlinear four-element Burger's model. Results from the above uniaxial tensile test and creep test show that the material behaviour is nonlinear. We have therefore extended the So–Chen NFEB model[8] to describe the mechanical behaviour of PR-MRC as follows.

(a) *Nonlinear spring element:* The relation between creep strain quantity Λ and engineering stress σ of the rubber elasticity

$$\sigma = 2a_1\left(\lambda - \frac{1}{\lambda^2}\right)\left(1 + \frac{a_2}{a_1}\frac{1}{\lambda}\right) = G\Lambda \tag{20}$$

$$\Lambda = \left(\lambda - \frac{1}{\lambda^2}\right)\left(1 + \frac{a_2}{a_1}\frac{1}{\lambda}\right); \quad \lambda = 1 + \epsilon \tag{21}$$

where λ is the stretch ratio and G is the shear modulus.

(b) *Nonlinear dashpot element:* When the material is under stress, this will result in slippage and frequent breakage of the atomic structure. Tobolsky and Eyring[10] derived a linear reaction rate formula from the micromolecular chain and energy barrier point of view, i.e.

$$\dot{\epsilon} = K\sinh(v\sigma) \tag{22}$$

By extending the above linear relation to a nonlinear relation we have

$$\dot{\Lambda} = A\sinh(v\sigma) \tag{23}$$

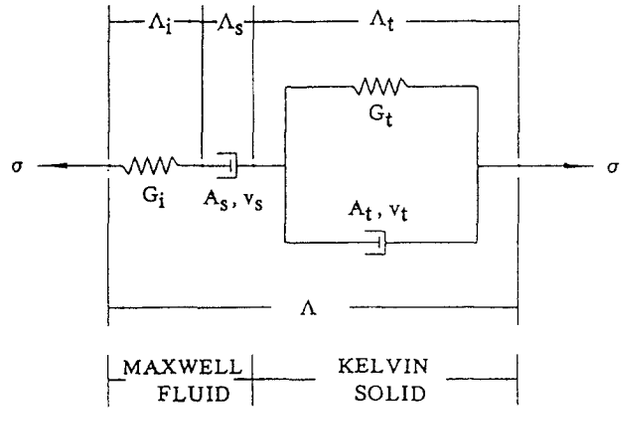

Figure 4 Nonlinear four-element Burger's model

with

$$A = K\exp\left(-\frac{\Delta H}{RT}\right) \tag{24}$$

where K and A relate to the activation energy, and v is the shift quantity of the energy barrier under stress or the activation volume; all these three constitute the activation mechanism index of the micromolecular chain. This NFEB model is shown in *Figure 4*.

Constitutive equations of the composites. The theory is developed for a material at a constant, elevated temperature. When the rubber matrix is subjected to a tensile stress σ, its total creep strain Λ and time-dependent deformation usually undergo both primary (transient) and secondary (steady-state) creep. The total nonlinear creep strain is

$$\Lambda = \Lambda_i + \Lambda_t + \Lambda_s \tag{25}$$

the three components of which can be expanded as follows.

(1) *Initial stretch* Λ_i

$$\Lambda_i = \frac{\sigma}{G_i} \tag{26}$$

(2) *Transient-stage creep rate*

After some manipulation we can rewrite $\dot{\Lambda}$ as

$$\dot{\Lambda}_t = \frac{2A_t\tanh(v_t\sigma/2)\exp(-v_tG_tA_tt)}{1 - [\tanh(v_t\sigma/2)\exp(-v_tG_tA_tt)]^2}$$

where

$$1 > [\tanh(v_t\sigma/2)\exp(-v_tG_tA_tt)]^2 \tag{27}$$

(3) *Steady-state creep rate* (Eyring reaction rate formula)

Here we assume that the time rate of change in the nonlinear stretch parameter also satisfies the Eyring equation for activated non-Newtonian viscous material.

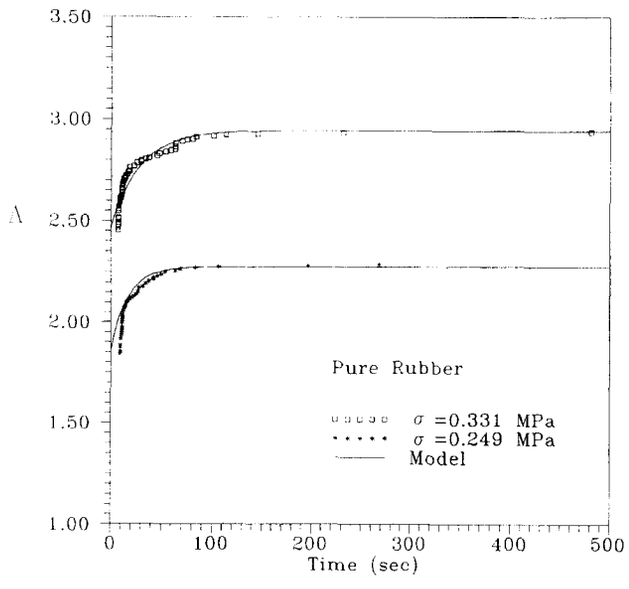

Figure 5 Creep history diagram for pure rubber

Then we obtain

$$\dot{\Lambda}_s = A_s \sinh(v_s \sigma) \tag{28}$$

Therefore, the total creep strain is

$$\Lambda(t) = \frac{\sigma}{G_i} + A_s t \sinh(v_s \sigma) + \frac{\sigma}{G_i}\left\{1 - \frac{2}{v,\sigma}\tanh^{-1}[\tanh(v_t\sigma/2)\exp(-v_t G_t A_t t)]\right\} \tag{29}$$

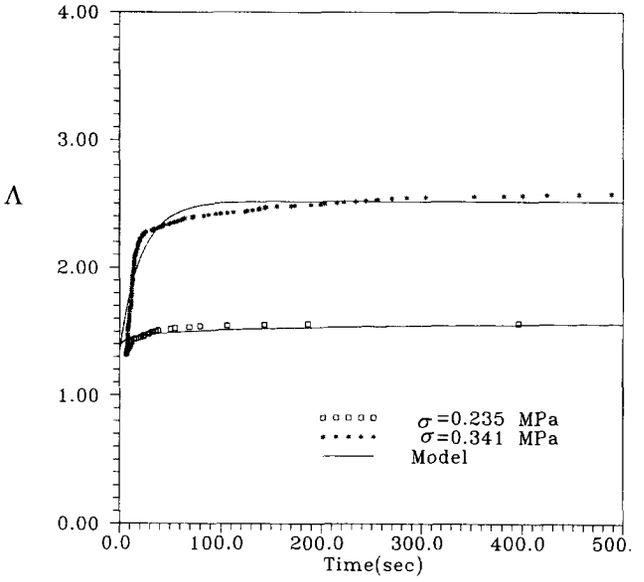

Figure 6 Creep history diagram for glass-beads-reinforced HTPB rubber composites

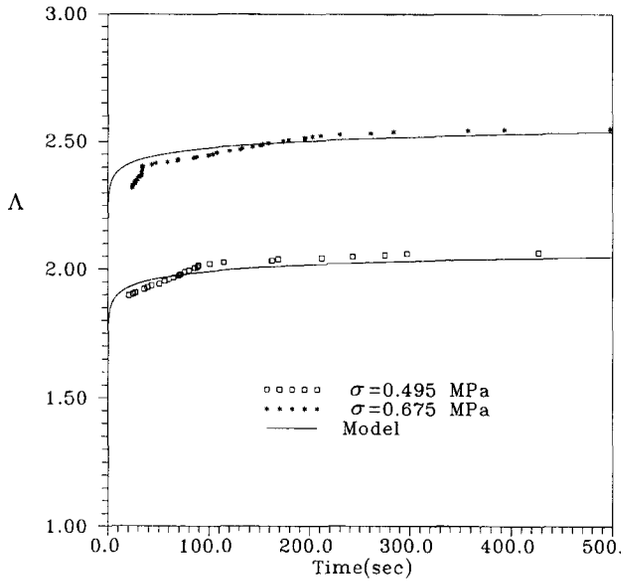

Figure 7 Creep history diagram for graphite-reinforced HTPB rubber composites

where G_i, G_t, A_s, A_t, v_s and v_t are the material constants which can be determined from creep experiments.

Determination of material constants (G_i, G_t, A_s, A_t, v_s *and* v_t). From creep test data, first, we transform the strain $\epsilon(t,\sigma)$ into $\Lambda(t,\sigma)$ by using equation (4), then determine the material constants from the Λ vs time curve. Theoretically, to find the six material constants only two creep strain vs time curves are needed. However, it is difficult to determine them simultaneously. Therefore, three steps are used to seek the material constants as follows:

(a) G_i is obtained from the initial value of the Λ vs time curve;
(b) two steady-stage creep strain curves are used to determine v_s, then the best least-square method is used to find A_s;
(c) the value of $(\sigma/G_i) + A_s t \sinh(v_s\sigma)$ is subtracted from $\Lambda(t)$, then the best least-square method is used to find G_t, A_t and v_t.

NFEB model and creep behaviour. *Figures 5–7* show typical creep stretch curves for the composites, where the solid lines are the NFEB model's predictions and symbols denote the experimental results. The six parameters for the solid lines in each figure can be computed from the data on any two creep curves in the same figure, and are listed in *Table 2*. They show that the NFEB model can well describe the composites' creep behaviour—initial stretch, transient-stage stretch and steady-state stretch. The results show that the curve is shifted upward as the stress is increased, which suggests that Λ increases with increasing loading stress σ. The creep stretch Λ decreases with increasing volume fraction f_1 of the inclusions, which is consistent with physical phenomena.

CONCLUSIONS

The main reason for the success of the proposed model is that we have clearly identified the basic element (mechanically coupled composite inclusion) which constitutes the particulate-filled rubber composites.

The initial stress–strain curves of the creep test coincide with the stress–strain curve of the uniaxial tensile test, suggesting that the theory of rubber elasticity can well describe the initial stress–strain behaviour of the creep test. Experimental results show that the Eyring reaction rate principle is a suitable description of steady-stage creep at a constant strain rate. This steady-stage creep occupies the most part of the whole creep history and the material fractures with no advance symptom.

The NFEB model, based on the entropy spring of the rubber elasticity and the Eyring reaction-rate principle, can well describe the whole creep history of the composites.

Table 2 The material constants of the NEFB model of equation (28)

Particles	f_1 (%)	G_i (MPa)	A_s (s^{-1})	v_s (MPa^{-1})	G_t (MPa)	A_t (s^{-1})	v_t (MPa^{-1})
	0	0.14	5.2×10^{-7}	0.1	1.01	8.4×10^{-5}	30
glass beads	10	0.16	5.8×10^{-7}	0.1	1.01	3.0×10^{-5}	30
graphite	23	0.33	9.0×10^{-8}	0.55	1.01	3.0×10^{-5}	30

ACKNOWLEDGEMENTS

The authors wish to express their thanks to Professor Yih-Hsing Pao for many helpful suggestions. This work is supported by the National Science Council of Taiwan, NSC-80-0405-E002-13.

REFERENCES

1 Nielsen, L. E. 'Mechanical Properties of Polymers and Composites', Marcel Dekker, New York, 1974
2 Ward, I. M. 'Mechanical Properties of Solid Polymers', 2nd edn, John Wiley & Sons, New York, 1983
3 Aklonis, J. J. and Macknight, W. J. 'Introduction to Polymer Viscoelasticity', 2nd edn, John Wiley & Sons, New York, 1983
4 Findley, W. N., Lai, J. S. and Onaran, K. 'Creep and Relaxation of Nonlinear Viscoelastic Materials—with an Introduction to Linear Viscoelasticity', North-Holland, New York, 1976
5 Christensen, R. M. 'Theory of Viscoelasticity', Academic Press, New York, 1982
6 Rivlin, R. S. *Rheol. Acta* 1983, **22,** 160
7 Schapery, R. A. *Polym. Eng. Sci.* 1969, **9,** 195
8 So, H. and Chen, Y. D. *Polym. Eng. Sci.* 1991, **31,** 410
9 Truesdell and Noll, 'The Nonlinear Field Theories of Mechanics' in 'Encyclopedia of Physics', (Ed. S. Flgge), Vol. 3, Springer-Verlag, Berlin, 1965
10 Saylak, D. and Beckwith, S. W. 'An Integral Approach to Solid Propellant Cumulative Damage', Air Force Rocket Propulsion Laboratory, UTEC, SI 69-070, 1969